Catalysis Letters 32 (1995) 205–213

Redox processes of surface of vanadyl pyrophosphate in relation to selective oxidation of *n*-butane

Gaku Koyano, Toshio Okuhara [1] and Makoto Misono

Department of Applied Chemistry, Faculty of Engineering, The University of Tokyo, Bunkyo-ku, Tokyo 113, Japan

Received 11 November 1994; accepted 1 February 1995

Oxidation and reduction processes of the surface of vanadyl pyrophosphate ($(VO)_2P_2O_7$) have been studied by means of Raman spectroscopy, X-ray photoelectron spectroscopy, thermogravimetry, and "micro-pulse" reaction of *n*-butane in relation to the selective oxidation of *n*-butane. Oxidation of $(VO)_2P_2O_7$ by O_2 was carried out to controlled extents by changing the reaction temperature and period. When $(VO)_2P_2O_7$ was oxidized at 733 K for 2 h, about one layer of the surface of $(VO)_2P_2O_7$ was oxidized to the X_1 phase, which was reported previously by the authors, as deduced from the amount of O_2-uptake and spectroscopic changes. Reductions of the surface X_1 phase and β-$VOPO_4$ were carried out by a "micro-pulse" reaction with *n*-butane at 733 K. The reduction by *n*-butane changed the surface X_1 phase to $(VO)_2P_2O_7$ and, at the same time, gave maleic anhydride with selectivities ranging from 13 to 40%. The selectivity was less than 10% in the case of β-$VOPO_4$. These results suggest that the redox cycle between the X_1 phase and $(VO)_2P_2O_7$ in the surface layer is involved in the catalytic oxidation of *n*-butane to maleic anhydride.

Keywords: selective oxidation of *n*-butane; redox mechanism; $(VO)_2P_2O_7$; X_1 phase

1. Introduction

$(VO)_2P_2O_7$ has been indicated to be the active component of the industrial catalyst for the production of maleic anhydride (MA) by the oxidation of *n*-butane [1–3]. Some researchers inferred that the single crystalline phase of $(VO)_2P_2O_7$ is the active phase of this reaction [4–6]. On the other hand, Volta et al. claimed that a biphasic catalyst consisting of $(VO)_2P_2O_7$ and γ-$VOPO_4$ is active [7] and Yamazoe et al. reported that a phosphorus-rich phase is efficient for this reaction [8].

Trifirò et al. have reported that $(VO)_2P_2O_7$ having rose-like crystallites is highly active [6a]. Since the (100) plane is the dominant surface of this rose-like $(VO)_2P_2O_7$, the active plane of $(VO)_2P_2O_7$ is thought to be (100), on which

[1] To whom correspondence should be addressed.

V^{4+}–O–V^{4+}(=O) pair sites are located. Bordes et al. have proposed on the basis of a crystallographic model that the (100) plane of $(VO)_2P_2O_7$ is efficient for the selective oxidation of *n*-butane [9]. The authors have demonstrated by using large plate-like crystallites of $(VO)_2P_2O_7$ that the (100) plane is selective for the formation of MA, while side planes ((001), (021), etc.) are active for non-selective oxidation [10].

It is generally accepted that the oxidation of *n*-butane over $(VO)_2P_2O_7$ takes place in its surface layer via a redox mechanism, i.e., Mars–van Krevelen mechanism [11], where the surface layer is oxidized to V^{5+} to a certain extent at the steady state of the reaction. Pepera et al. [12] and the authors [13] showed by the experiments using $^{18}O_2$ that the diffusion of oxygen atoms during the reaction is limited to only a few surface layers. Thus, the structure and redox property of the surface V^{5+} phase are important for this reaction. Various phases of V^{5+} have already been reported: β-$VOPO_4$ [14], α-$VOPO_4$ [15], X_1 phase [4], γ-$VOPO_4$ [16], δ-$VOPO_4$ [16], β′ phase [17], and β″ phase [17]. Since X_1, δ and β″ phases gave very similar X-ray diffraction (XRD) patterns [4,16,17], these are possibly identical. The valency of vanadium in the X_1 phase was reported to be close to 5 [4]. The X_1 phase is soluble in water, while β-$VOPO_4$ is insoluble [4,18].

In the present study, changes in the surface phase of $(VO)_2P_2O_7$ upon the oxidation with O_2 or reduction with *n*-butane have been mainly investigated with Raman spectroscopy. Here, we wish to report that the X_1 phase is involved in a redox process with the surface phase of $(VO)_2P_2O_7$.

2. Experimental

$(VO)_2P_2O_7$ was obtained by the treatment of the precursor, $VOHPO_4 \cdot 0.5H_2O$, at 823 K in an N_2 flow for 5 h, where the precursor was prepared by the organic solvent method using benzyl alcohol, isobutyl alcohol, V_2O_5, and H_3PO_4 [6]. The BET surface area of $(VO)_2P_2O_7$ was 78 $m^2\ g^{-1}$. It was confirmed by SEM that $(VO)_2P_2O_7$ obtained in the present study had rose-like shape. The thickness along the (100) plane was estimated from the linewidth of the XRD peak to be about 100 Å, which corresponds to about 10 layers of $(VO)_2P_2O_7$ unit. Bulk X_1 phase (28 $m^2\ g^{-1}$) was synthesized from NH_4HVPO_6, which was obtained from $NH_4H_2PO_4$ and V_2O_5 as described previously [4]. β-$VOPO_4$ (3.2 $m^2\ g^{-1}$) was prepared by the calcination of $VOHPO_4 \cdot 0.5H_2O$ at 873 K in an O_2 flow for 10 h. The structure of these V–P oxides was confirmed with XRD.

After the $(VO)_2P_2O_7$ sample was pretreated in He at 773 K for 1 h in a flow system, O_2 (1 atm) was fed at a rate of 60 $cm^3\ min^{-1}$ for 2 h at 733–773 K. In order to determine the uptakes of oxygen during the O_2 treatment, the same experiment was repeated in a microbalance (Seiko Instruments, TG/DTA220), where the uptakes of oxygen were measured by the weight increase. The oxidation state of the catalyst is expressed in the following two ways; x in $V^{4+}_{1-2x}V^{5+}_{2x}PO_{4.5+x}$

(= $VPO_{4.5+x}$) and the number of V^{5+} layers (abbreviated as NL). The latter is the ratio of the number of V^{5+} to the number of vanadium atoms ($V^{4+} + V^{5+}$) in the surface monolayer of $(VO)_2P_2O_7$. The number of vanadium atoms in the surface monolayer was estimated to be 8.1×10^{-4} mol g^{-1} from BET surface area and the lattice parameters [19].

Raman spectra were taken with a laser Raman spectrometer (Jasco Corporation, NR-1800) using the 514.5 nm line from Ar ion laser (NEC GLS3261J). XPS (X-ray photoelectron spectroscopy) spectra were recorded with a Jeol JPS-90-SX spectrometer with Al Kα radiation, where samples were pressed into 10 mm disks. All spectra were referenced to the O 1s binding energy of 532 eV.

A "micro-pulse" reaction was performed in a pulse-reactor system equipped with a quadrupole mass spectrometer at the outlet of the reactor. After the catalysts were treated in He (60 ml min^{-1}) at 773 K for 1 h, a pulse of *n*-butane (0.71 cm^3 of 2.0% *n*-butane in He; *n*-butane = 6.0×10^{-7} mol) was injected repeatedly at intervals of about 1 min. The composition of maleic anhydride at the outlet was estimated using the peak intensity of $m/z = 54$ after the subtraction of the contributions resulting from fragmentation of *n*-butane, butenes, and butadiene. The compositions of *n*-butane, butenes, butadiene, furan, CO, and CO_2 were also calculated from the relative peak intensities of $m/z = 28$, 39, 41, 43, 44, 54, and 68. Sensitivity factors of these gases for the mass spectrometric analysis were determined separately for each gas.

3. Results and discussion

Fig. 1 shows the changes of Raman spectra of $(VO)_2P_2O_7$ upon the oxidation with O_2. The parent $(VO)_2P_2O_7$ gave a single peak at 923 cm^{-1}, which is consistent with the literature [5]. Moser and Schrader assigned this peak to ν(P–O–P) of the P_2O_7 group [20]. As shown in fig. 1b, when $(VO)_2P_2O_7$ was oxidized at 733 K for 2 h ($x = 0.047$, NL = 0.94), a strong peak at 937 cm^{-1} and weak peaks at 1020, 1075, and 1090 cm^{-1} appeared in addition to the peak at 923 cm^{-1}. Further oxidation at 773 K for 2 h ($x = 0.25$, NL = 4.9) (fig. 1c) gave a pattern having four peaks at 937, 1020, 1075, and 1090 cm^{-1} together with peaks at low wave numbers (655, 590 and 550–380 cm^{-1}). This spectrum (fig. 1c) is in good agreement with that of bulk X_1 phase, with a small contribution from $(VO)_2P_2O_7$ (fig. 1d). As shown in fig. 1e, β-$VOPO_4$ gave distinct peaks at 896, 987, and 1072 cm^{-1} as well as the peaks having low wave numbers as noted in the literature [20]. None of these peaks were detected for the oxidized $(VO)_2P_2O_7$. The spectrum of X_1 phase is also different from that of α-$VOPO_4$ reported in the literature [20]. Therefore it is evident that the phase formed by the controlled oxidation of $(VO)_2P_2O_7$ is the X_1 phase. The peak at 937 cm^{-1} has been assigned to $\nu(PO_4)$, and the peaks at 1075 and 1090 cm^{-1} of the X_1 phase to ν(V–O–P) [21]. The peaks below 700 cm^{-1} are probably due to the bending modes and coupled vibrations of the crystal lattice [21].

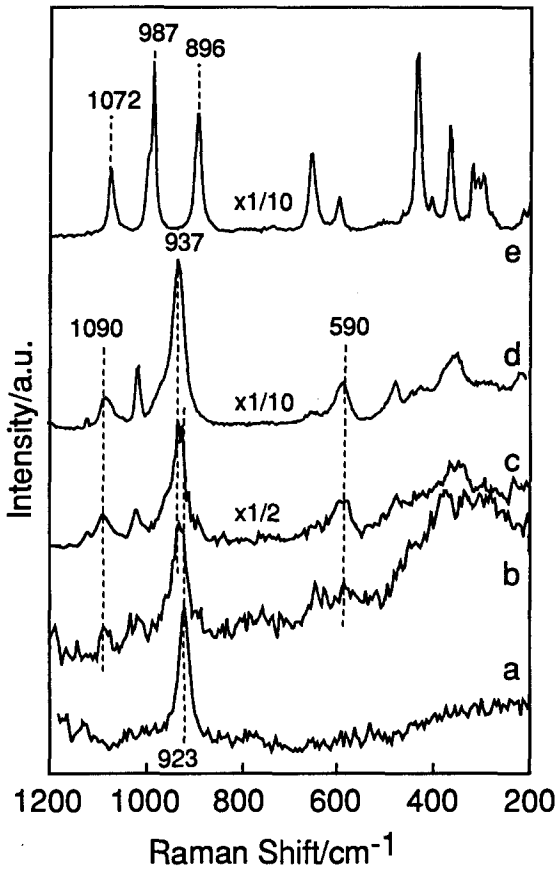

Fig. 1. Raman spectra of (a) $(VO)_2P_2O_7$ before oxidation, (b) $(VO)_2P_2O_7$ after oxidation at 733 K ($x = 0.047$, NL = 0.94), (c) $(VO)_2P_2O_7$ after oxidation at 773 K ($x = 0.25$, NL = 4.9), (d) bulk X_1 phase, and (e) β-$VOPO_4$. x: x in $V^{4+}_{1-2x}V^{5+}_{2x}PO_{4.5+x}$ ($(VO)_2P_2O_7$ ($x = 0$), $VOPO_4$ ($x = 0.5$)); NL: number of V^{5+} layers (see text).

As shown in figs. 1a and 1d, the intensity of the peak (937 cm^{-1}) due to the X_1 phase is about 10 times greater than that (923 cm^{-1}) of $(VO)_2P_2O_7$, although the sample weights were the same. The great difference in peak intensity between these samples was confirmed for mechanical mixtures of $(VO)_2P_2O_7$ and bulk X_1 phase with different compositions. Therefore, the reason why the peak of X_1 phase was more intense than that of $(VO)_2P_2O_7$ in fig. 1b, in spite of a rather small degree of oxidation ($x = 0.047$), is probably this difference in sensitivity.

Raman spectroscopy gives information relating to the bulk of a sample [22]. On the other hand, XPS is concerned with only a few layers of the surface. Thus, we used XPS to determine whether the X_1 phase is formed on the surface or in the bulk. As shown in fig. 2a, the parent $(VO)_2P_2O_7$ gave peaks at 524.8 and 517.7 eV as in the literature [20], which are assignable to V $2p_{1/2}$ and V $2p_{3/2}$ of V^{4+} on $(VO)_2P_2O_7$, respectively. For the bulk X_1 phase, peaks at 526.4 and 518.9 eV were

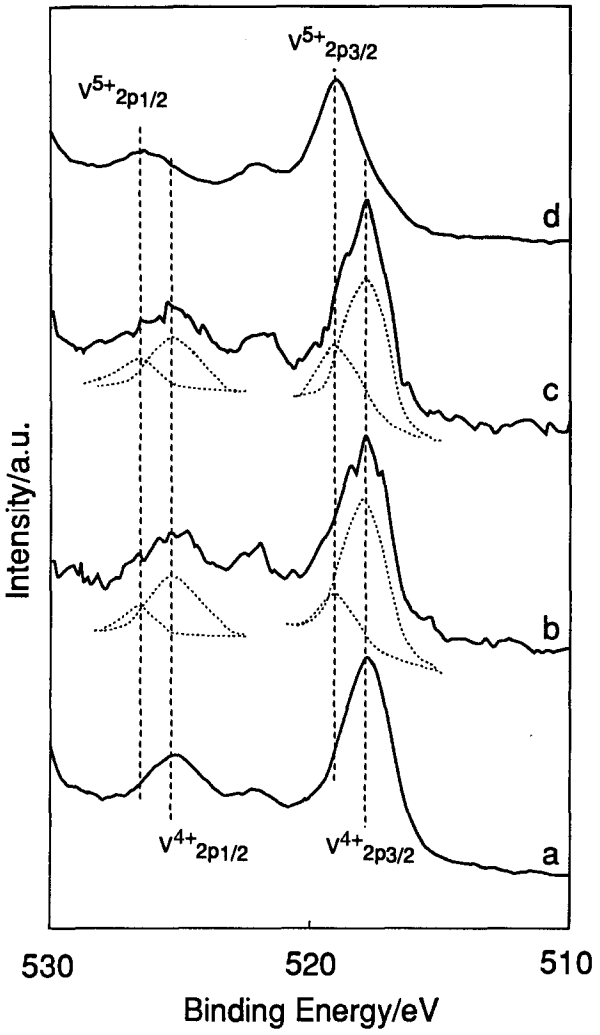

Fig. 2. XPS spectra of (a) $(VO)_2P_2O_7$ before oxidation, (b) $(VO)_2P_2O_7$ after oxidation at 733 K ($x = 0.047$, NL = 0.94), (c) $(VO)_2P_2O_7$ after oxidation at 753 K ($x = 0.80$, NL = 1.6), and (d) bulk X_1 phase. For (b) and (c), each spectrum was obtained by one scan to avoid the reduction during the measurement. x: x in $V^{4+}_{1-2x}V^{5+}_{2x}PO_{4.5+x}$; NL: number of V^{5+} layers (see text).

observed, which correspond to V $2p_{1/2}$ and V $2p_{3/2}$ of V^{5+}, respectively (fig. 2d). These peak positions were the same as for V^{5+} of β-$VOPO_4$ [23]. When $(VO)_2P_2O_7$ was oxidized at 733 K ($x = 0.047$, NL = 0.94) and 753 K ($x = 0.080$, NL = 1.6), the V $2p_{1/2}$ and V $2p_{3/2}$ peaks became broader due to the overlapping of the peaks due to V^{5+}. The ratio of the peak intensity for V^{5+} and V^{4+} ($I_{V^{5+}}/I_{V^{4+}}$) was determined to be 0.24–0.29 (oxidized at 733 K, fig. 2b) and 0.54–0.61 (oxidized at 753 K, fig. 2c) by the deconvolution of the peaks, assuming that the peak shape is the mean of a Lorentzian and Gaussian function and that each peak position and

width are unchanged (dotted curves in fig. 2). If the whole bulk was oxidized uniformly, $I_{V^{5+}}/I_{V^{4+}}$ should be equal to the bulk V^{5+}/V^{4+} ratio. The values ($I_{V^{5+}}/I_{V^{4+}}$) calculated for the case of bulk oxidation were 0.10 and 0.19 after the oxidations at 733 and 753 K, respectively, as calculated from the amount of O_2 uptake. The experimental values from XPS are significantly greater than the bulk values calculated, indicating that the bulk was not oxidized uniformly.

For further confirmation, the ratio of the XPS peak intensity was estimated by assuming that $(VO)_2P_2O_7$ was oxidized stepwise from the surface inward to form a V^{5+} surface phase. The estimation was carried out according to a model similar to that described in the literature [24]. The data of Scofield [25] ($\sigma_{V^{5+}} \approx \sigma_{V^{4+}} = 6.33$) for the photoionization cross-section of V^{5+} and V^{4+} were used. The mean free path of the photoelectron (λ) was calculated to be 13.5 Å, according to the method of Penn [26]. Densities of V^{5+} and V^{4+} ($n_{V^{5+}} = 1.2 \times 10^{-2}$ Å^{-3}, $n_{V^{4+}} = 1.3 \times 10^{-2}$ Å^{-3}) and the thickness of an ideal V^{5+} phase monolayer ($t = 4.1$ Å) were determined from the lattice parameters [17,19]. The ratios of $I_{V^{5+}}/I_{V^{4+}}$ according to this model were 0.31 and 0.57 at $x = 0.047$ (733 K) and $x = 0.080$ (753 K), respectively, which is in good agreement with the experimental values (0.24–0.29 (733 K) and 0.54–

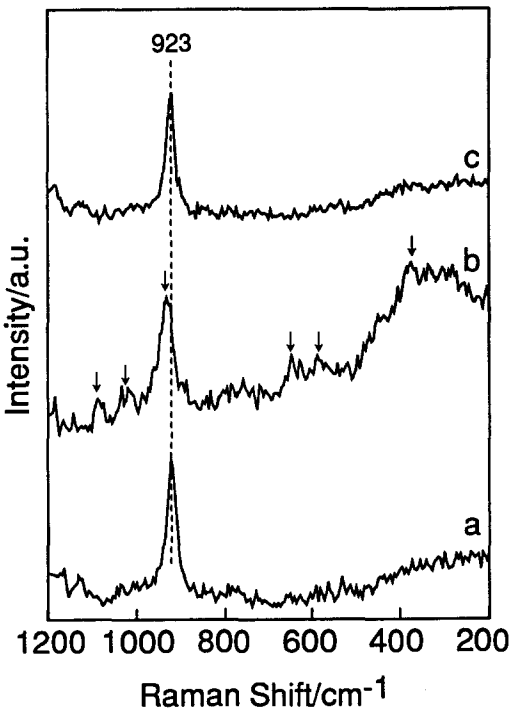

Fig. 3. Raman spectra of (a) $(VO)_2P_2O_7$ before oxidation, (b) $(VO)_2P_2O_7$ after oxidation at 733 K ($x = 0.047$, NL = 0.94), (c) after the pulse reaction of *n*-butane over the oxidized $(VO)_2P_2O_7$. Catalyst: about 200 mg (surface V = 1.3×10^{-5} mol). Pulse size of *n*-butane = 6.0×10^{-7} mol. A total of 34 pulses of *n*-butane was introduced at 733 K. Arrows show the peak positions for the X_1 phase.

0.61 (753 K)). Thus, it may be concluded that the oxidation occurred within the first few surface layers of $(VO)_2P_2O_7$.

Fig. 3 gives the Raman spectra before and after the micro-pulse reaction between *n*-butane and the surface X_1 phase, which was formed by preoxidation of $(VO)_2P_2O_7$ at 733 K. When pulses of *n*-butane (6.0×10^{-7} mol) were injected 34 times repeatedly to the surface X_1 phase, Raman peaks due to the X_1 phase gradually disappeared and the peak due to $(VO)_2P_2O_7$ was recovered (fig. 3c). This result shows that the surface X_1 phase was reduced by *n*-butane to $(VO)_2P_2O_7$. In fig. 4, the conversion of *n*-butane and the selectivity to MA during this pulse reaction are plotted against x in $VPO_{4.5+x}$, where x was calculated from the conversion of *n*-butane and the composition of the products according to Pepera et al. [12]. It was confirmed that the conversion of *n*-butane was very low (less than 8%) at the first pulse and was nearly zero after the fourth pulse for the $(VO)_2P_2O_7$ phase. When *n*-butane was pulsed to the surface X_1 phase, the conversion at the first pulse was more than 80%. It is remarkable that MA was formed with selectivities of 13–40% during the pulse reaction, together with CO and CO_2. In other words, the surface X_1 phase transformed *n*-butane to MA. The selectivity tended to increase as the surface oxidation state decreased (fig. 4). It is noteworthy that quite high selectivities were observed for the partially reduced surface X_1 phase. On the other hand, as

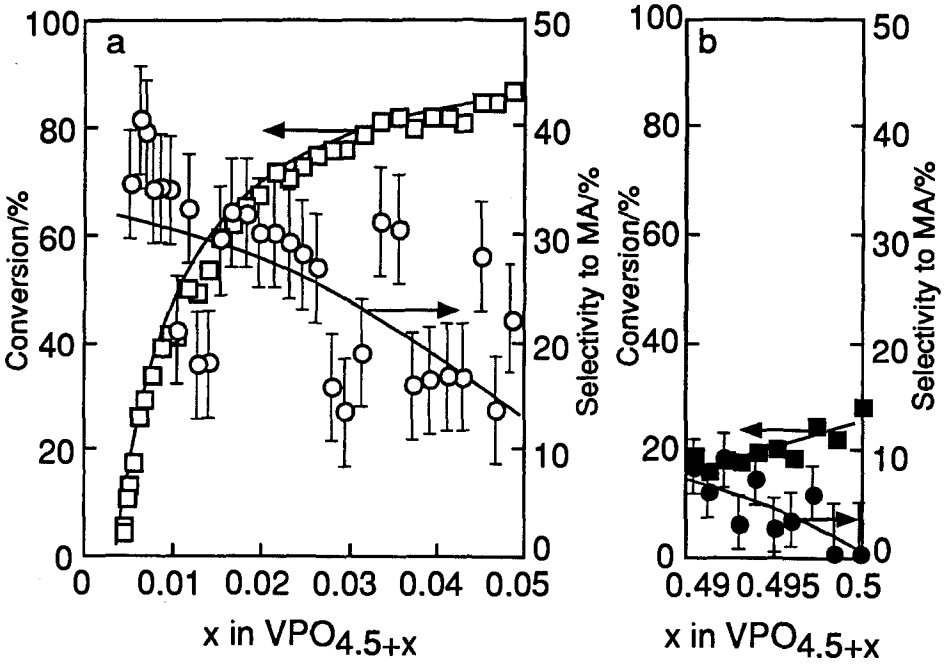

Fig. 4. Conversion of *n*-butane and selectivity to maleic anhydride for the pulse reaction of *n*-butane at 733 K. (a) $(VO)_2P_2O_7$ oxidized at 733 K, $x = 0.047$, (□) conversion, (○) selectivity to MA, catalyst weight: 200 mg; (b) β-$VOPO_4$, (■) conversion, (●) selectivity to MA, catalyst weight: 800 mg. Pulse size of *n*-butane = 6.0×10^{-7} mol. Flow rate of He: 60 cm^3 min^{-1}.

shown in fig. 4, β-$VOPO_4$ gave much lower selectivities (always less than 10%), which is consistent with the result of the catalytic reaction [4]. When the pulses of *n*-butane were introduced to the bulk X_1 phase at 733 K, the selectivities to MA were in the range from 15 to 30%, which is comparable to the surface X_1 phase.

Therefore, it may be concluded that the X_1 phase is involved in the redox cycle of the surface of $(VO)_2P_2O_7$ during the oxidation of *n*-butane to MA and the reaction proceeds on a partially-reduced X_1 phase. As for the structure of the X_1 phase, from the analogy of XRD patterns between $(VO)_2P_2O_7$ and the β″-phase (X_1 phase), Matsuura et al. claimed that the β″-phase has a V–V dioctahedral structure [17]. On the other hand, Volta et al. presumed, from a Raman spectroscopic study, that the vanadium atoms of δ-$VOPO_4$ (= X_1 phase) are in isolated octahedra [18]. Our preliminary EXAFS results for the X_1 phase clearly show that V–V pair sites are present in the X_1 phase [27]. Details about the changes of the structure during the oxidation–reduction processes will be discussed in a forthcoming paper.

References

[1] G. Centi, F. Trifirò, J.R. Ebner and V.M. Franchetti, Chem. Rev. 88 (1988) 55.
[2] B.K. Hodnett, Catal. Rev. Sci. Eng. 27 (1985) 373.
[3] G. Centi, Catal. Today 16 (1993) 5.
[4] T. Shimoda, T. Okuhara and M. Misono, Bull. Chem. Soc. Jpn. 58 (1985) 2163.
[5] T.P. Moser and G.L. Schrader, J. Catal. 92 (1985) 216.
[6] (a) G. Busca, F. Cavani, G. Centi and F. Trifirò, J. Catal. 99 (1986) 400;
(b) US Patent 4,392,986 (1987) to Exxon Res. Eng. Co., T.C. Yang, K.K. Rao, I. Der Huang.
[7] F.B. Abdelouahab, R. Olier, N. Guilhaume, F. Lefebvre and J.C. Volta, J. Catal. 128 (1991) 248.
[8] H. Morishige, J. Tamaki, N. Miura and N. Yamazoe, Chem. Lett. (1990) 1513.
[9] J. Ziolotlowski, E. Bordes and P. Courtine, J. Mol. Catal. 84 (1993) 307.
[10] (a) T. Okuhara, K. Inumaru and M. Misono, *Catalytic Selective Oxidation*, ACS Symp. Ser. 523 (Am. Chem. Soc., Washington, 1993) p. 156;
(b) K. Inumaru, T. Okuhara and M. Misono, Chem. Lett. (1992) 1955.
[11] P. Mars and D.W. van Krevelen, Chem. Eng. Sci. 3 (1954) 41.
[12] M. Pepera, J.L. Callahan, M.J. Desmond, E.C. Milberger, P.R. Blum and N.J. Bremer, J. Am. Chem. Soc. 107 (1985) 4883.
[13] M. Misono, K. Miyamoto, K. Tsuji, T. Goto, N. Mizuno and T. Okuhara, *New Developments in Selective Oxidation*, Stud. Surf. Sci. Catal. (Elsevier, Amsterdam, 1990) p. 605.
[14] R. Gopal and C. Calvo, J. Solid State Chem. 5 (1972) 432.
[15] B. Jordan and C. Calvo, Can. J. Chem. 51 (1972) 2621.
[16] E. Bordes and P. Courtine, J. Chem. Soc. Chem. Commun. (1985) 294.
[17] I. Matsuura, A. Mori and M. Yamazaki, Chem. Lett. (1987) 1897.
[18] F.B. Abdelouahab, J.C. Volta and R. Olier, J. Catal. 148 (1994) 334.
[19] Y.E. Gorbunova and S.A. Linde, Sov. Phys. Dokl. 24 (1979) 138.
[20] T.P. Moser and G.L. Schrader, J. Catal. 104 (1987) 99.
[21] F.B. Abdelouahab, R. Olier, N. Guilhaume, F. Lefebvre and J.C. Volta, J. Catal. 134 (1992) 151.
[22] H. Morishita, T. Ishioka, M. Kobayashi and K. Sato, J. Phys. Chem. 91 (1987) 2273.

[23] H. Igarashi, K. Tsuji, T. Okuhara and M. Misono, J. Phys. Chem. 97 (1993) 7065.
[24] K. Inumaru, T. Okuhara and M. Misono, J. Phys. Chem. 95 (1991) 4826.
[25] J.H. Scofield, J. Electron Spectry. Relat. Phenom. 8 (1976) 129.
[26] D.R. Penn, J. Electron Spectry. Relat. Phenom. 9 (1976) 29.
[27] G. Koyano, F. Yamaguchi, T. Okuhara and M. Misono, 74th Annual Meeting of Catalysis Society of Japan, 3B03 (1994).